# Numerical modeling of the fire behavior of composite steel and concrete joints after earthquake

Thiago Pires[1,*], João Paulo C. Rodrigues[1,2,3;#] Ruben R. Lopes[2,3;$]

[1] *Federal University of Minas Gerais, Department of Structural Engineering, Belo Horizonte, Brazil*
[*]thiagopires@ufmg.br
[2] *University of Coimbra, CERIS, Department of Civil Engineering, Coimbra, Portugal.*
[3] *Itecons, Coimbra, Portugal.*
[#]jpaulocrod@ufmg.br
[$]ruben.lopes@itecons.uc.pt

**Abstract.** This paper presents a numerical model for analyzing the fire behavior of composite steel and concrete end-plate joints after earthquake. The model was developed and validated with experimental results. The obtained moment-rotation results showed that cyclic loading damage affects the performance of the joint in case of fire.

**Keywords:** post-earthquake fire, numerical simulation, joint, steel, concrete.

## 1 Introduction

Post-earthquake fires (PEF) are extreme events considered of low-probability, but they can cause severe damages to buildings and consequently endanger the lives of their occupants. Regrettably, some cases have already been reported worldwide. One of the earliest documented cases occurred in Lisbon, on november 1st, 1775, where the city was devastated by a fire subsequent to an earthquake. According to historians, the earthquake's magnitude may have ranged from 8.5 to 9.0, and the fire outbreak could be attributed to the prevalent use of fireplaces and candles during that time [1]. In Tokyo, the event known as Great Kanto Earthquake, in 1923, was one of the worst natural disasters in the history of Japan. According to Schencking [2], around 130 fires were recorded in the first thirty minutes after the earthquake. Approximately, 92.000 deaths were reported due to fires, representing 90% of the total. In US, in April 1995, San Francisco was struck by a 7.8 magnitude earthquake. According to the National Archieve [3] the post-earthquake fire killed more than 3.000 people and destroyed about 100.000 buildings. Another disaster in Japan was the 6.8 magnitude earthquake that occurred in 1995 near the port of Kobe, which is approximately 500 km southwest of Tokyo. The National Fire Protection Association (NFPA) [4] reported that the earthquake and ensuing fire destroyed over 100,000 buildings and claimed more than 6,000 lives. More recently, a seismic event with a magnitude of 9.1 on the Richter scale struck the Fukushima region, leading to significant impacts on the operations of the nuclear power plant. The seismic activity triggered failures in the plant's cooling system, resulting in several explosions and fire outbreaks. The most notable fire incident occurred in the fourth reactor building, where a hydrogen explosion causing a large fire that burned for several days [5].

Those events demonstrate the destruction potential of post-earthquake fires, which are often more devastating than the earthquake itself. This is due to a combination of factors, such as disruption of power supply lines, leakage of flammable materials and damage to structures. Furthermore, the emergency services such as fire departments, hospitals and police stations are often overwhelmed, making the fight against fire even more challenging. In recent years, some research has focused on the study of steel framed structures and their behaviour during earthquakes and post-earthquake fires. The study of structural joints helps to understand how buildings behave during those events and allows to ensure people's safety.

Tartaglia et al. [6] developed a numerical model to investigate the behaviour of extended stiffened end-plate joints at elevated temperatures after seismic action. The aim was to evaluate the influence of the seismic damage on the performance of this type of joint in high fire conditions. Xu et al. [7] have examined end-plate joints with column web stiffeners and considered different earthquake damages and their influence on fire resistance. Song et al. [8] conducted an experimental test to investigate the behavior of a welded steel I-beam to a hollow column joint in a post-earthquake fire situation. The joint consisted of a 200 x 200 mm column and a 131.6 x 203 mm I-beam, grade 250 and grade 350 steel, respectively. Song et al. [8] observed the material hardening in the experimental tests when the joint was subjected to small cyclic loading amplitude.

In the actual work it is presented a model for composite steel and concrete joints subjected to fire after earthquake. The numerical model was deloped in Abaqus. Moment capacity, rotation, and failure modes were determined and compared with experimental results.

# 2 Finite element analysis

In this study, the finite element software Abaqus/CAE was used to obtain an efficient model for predicting the behavior of the joint subject to fire after seismic loading. For validating the numerical model, the results have been compared with experimental results reported by Barata et al. [9] and numerical results reported by Matias et al. [10]. Material nonlinearities have been considered. All aspects of the model developed are presented in the following sections.

## 2.1 Model Geometry

Fig. 1 shows the geometry of the model used by Barata et al. [9] on their experimental tests. The setup consisted of a IPE270 beam connected to a HEA240 column carrying a composite slab. The joint beam-to-column was made by a 12 mm thickness endplate and 6 M20 high-strength bolts.

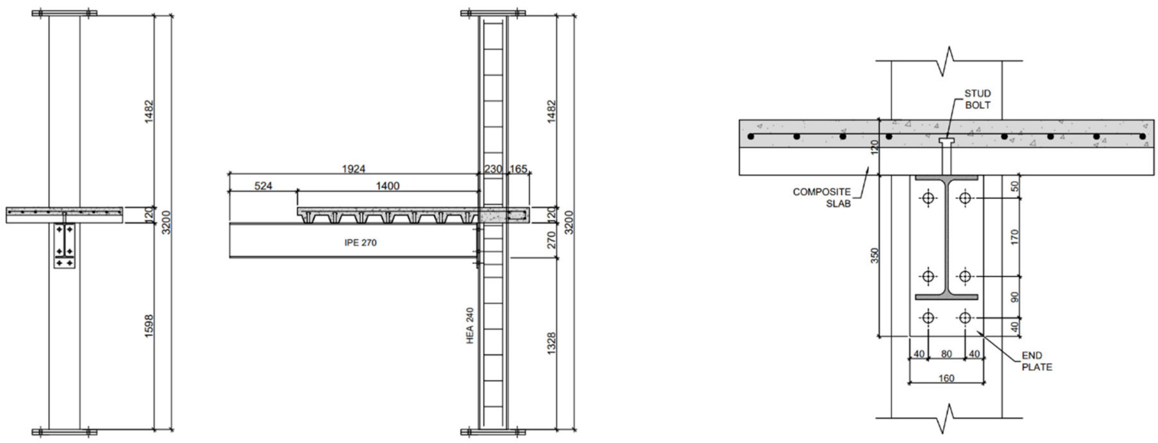


Figure 1. Geometry of the experimental model used in the numerical model [9]

## 2.2 Finite element type and mesh

The solid elements such as steel beam, composite colum, composite slab, high-strength bolts, stud bolts and steel deck were represented using the C3D8R (8-node linear brick), while the linear elements, such as slab and column reinforcing bars, were represented using T3D2 (2-node linear). For high-temperature analysis, C3D8T field-variable-dependent conductivity elements have been used.

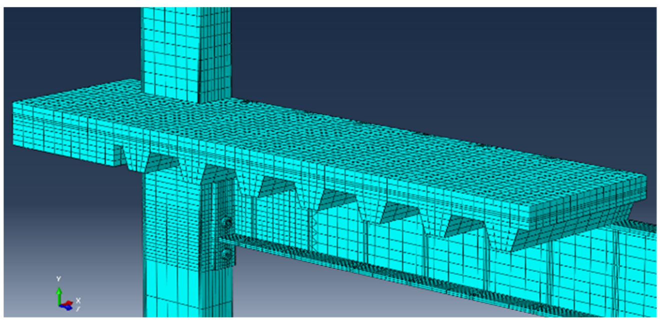

Figure 2. Meshed model for the composite joint

The mesh was refined near the joint and the reduced integration present in Abaqus was used. The sensitivity analysis was performed specially in the concrete slab, which the behavior is impacted by the size of the elements of the mesh. The mesh size used in the slab and end-plate was 25 mm and in the high-strength bolts was 1.0 mm. Beam and composite column were refined near the joint with 20 and 15 mm element size, respectively. Fig. 2 shows the meshed model.

## 2.3 Contact modeling

The interaction between the model elements was done using surface-to-surface contact. For this type of contact, tangential and normal behavior were defined at ambient temperature. Tangential behavior was defined using the classical Coulomb friction with a coefficient of 0.35 for steel-steel contact and 0.7 between the concrete and steel deck in the slab. Normal behavior was defined with 'hard contact'. This type of contact does not allow any penetration. To simulate the weld between the beam-endplate and the beam-stud bolt, a tie constraint was used. For high-temperature analysis, a thermal conductance parameter was added in all contacts, with a conductance value of 200 W/m.K [10].

## 2.4 Material Modeling

The model presents five structural steels, each assigned to specific elements. Steel beam, end plate and steel column, have been modeled using a stress-strain relationship defined in EN 1993-1-2 [11] for steel grade S355. High-strength bolts, grade 8.8, have been modeled using the Hanus et al. [12] stress-strain relationship, with $f_y$ and $f_u$ values extracted from Ketabdari et al. [13]. Stud bolt connectors have been simulated according to the relationship proposed by EN 1993-1-2 [11] with experimental results by Matias et al. [10]. The slab and column reinforcing bars have been modeled using parameters provided in EN 1992-1-2 [14], and steel deck was designed according to EN 1993-1-2 [11]. Tab. 1 lists the mechanical properties of these structural elements.
The behavior of concrete in compression was defined according to EN 1992-1-2 [14] with $f_{ck}$ = 20 MPa, $E$ = 30GPa, $v$ = 0.3 and $f_{ctm}$ = 2.21 MPa. In tension, the behavior was defined using a stress-displacement relationship based on fracture energy proposed by Silva [15]. Concrete Damaged Plasticity model (CDP) presented in Abaqus was used to determine the inelastic behavior of concrete. The inelastic parameters used in CDP model were taken from Bolina [16].

Table 1. Mechanical properties as a function of temperature

| Temp (°C) | Beam, Column, End plate | | | High-Strenght Bolt | | | Reinforcing Bar | | | Stud-Bolt | | | Steel-deck | | |
|---|---|---|---|---|---|---|---|---|---|---|---|---|---|---|---|
| | $f_y$ (MPa) | $f_u$ (MPa) | E (GPa) | $f_y$ (MPa) | $f_u$ (MPa) | E (GPa) | $f_y$ (MPa) | $f_u$ (MPa) | E (GPa) | $f_y$ (MPa) | $f_u$ (MPa) | E (GPa) | $f_y$ (MPa) | $f_u$ (MPa) | E (GPa) |
| 20 | 355 | 490 | 200 | 871 | 968 | 190 | 500 | 500 | 200 | 400 | 400 | 200 | 280 | 280 | 200 |
| 100 | 355 | 490 | 200 | 796 | 937 | 190 | 500 | 500 | 200 | 400 | 400 | 200 | 280 | 280 | 200 |
| 200 | 355 | 444 | 180 | 724 | 905 | 171 | 405 | 500 | 174 | 324 | 400 | 174 | 226 | 280 | 180 |
| 300 | 355 | 444 | 160 | 677 | 874 | 152 | 305 | 500 | 144 | 244 | 400 | 144 | 172 | 280 | 160 |
| 400 | 355 | 355 | 140 | 563 | 750 | 133 | 210 | 500 | 112 | 168 | 400 | 112 | 118 | 280 | 140 |
| 500 | 277 | 277 | 120 | 399 | 532 | 114 | 180 | 390 | 80 | 144 | 312 | 80 | 101 | 218 | 120 |
| 600 | 167 | 167 | 62 | 160 | 213 | 59 | 90 | 235 | 48 | 72 | 188 | 48 | 50 | 132 | 62 |
| 700 | 82 | 82 | 26 | 65 | 97 | 25 | 35 | 115 | 16 | 28 | 92 | 16 | 21 | 64 | 26 |
| 800 | 39 | 39 | 18 | 39 | 65 | 17 | 25 | 55 | 12 | 20 | 44 | 12 | 14 | 31 | 18 |
| 900 | 21 | 21 | 14 | 19 | 32 | 13 | 20 | 30 | 10 | 16 | 24 | 10 | 11 | 17 | 14 |
| 1000 | 14 | 14 | 9 | | | | 10 | 20 | 6 | 8 | 16 | 6 | 7 | 11 | 9 |

For high temperature analysis, thermal properties of the materials have been used according to EN 1993-1-2 for steel and EN 1992-1-2 for concrete elements. The emissivity value adopted was 0.7 and the film coefficient was 25 W/m² for all materials.

## 2.5 Loading and boundary conditions

Table 2 presents the loading cases used in the experimental and numerical models. The first two simulations, positive monotonic and negative monotonic, E1 and E2, were designed to determine the joint's elastic parameters and resistance capacity. The obtained parameters were used to conduct the test E3, which involved applying cyclic loading at ambient temperature according to European Convention for Constructional Steelwork – ECCS Tecnicla Note nº 45 [17]. The loading cases, E4, E5 and E6, were conducted to evaluate the behavior of the joint under high temperatures followed by seismic (cyclic) loading. The testing procedure involved applying cyclic loading according to the ECCS Technical Note 45 [17], followed by a constant loading of 27kN, which represents 30% of the ultimate loadbearing capacity of the joint at ambient temperature. The specimens were then subjected to temperatures up to 600°C, following approximately the standard temperature-time fire curve ISO 834, before load increments have been applied until joint failure occurred.

Table 2. Loading cases used in the experimental and numerical program.

| Group | Test | 1st stage | 2nd stage | 3rd stage |
|---|---|---|---|---|
| A | E1 | Monotonic ($M^-$) | - | - |
| | E2 | Monotonic ($M^+$) | - | - |
| | E3 | Cyclic Loading | Monotonic ($M^-$) | - |
| B | E4 | Cyclic Loading | Monotonic ($M^-$) | Heating up to failure |
| | E5 | Cyclic Loading | Heating up to 600°C | Combination $M^-$ - $M^+$ |
| | E6 | Cyclic Loading | Heating up to 600°C | Combination $M^-$ - $M^+$ |

# 3 Validation of the model

## 3.1 Ambient temperature results

The numerical results for moment-rotation at ambient temperature for E1 and E2 cases are compared to experimental results in Fig. 3, respectively. The load carrying capacity and initial stiffness of the steel joint were in very close agreement with the experimental results. The maximum moment observed during the experiment E1 was 161 kN.m and the one predicted by the numerical model was 170 kN.m. The error between the values of maximum load carrying capacity was 5.1%. For the experiment E2, the maximum moment observed during the test was 223 kN.m and numerical model was 229 kN.m, with a difference of 2.6 %

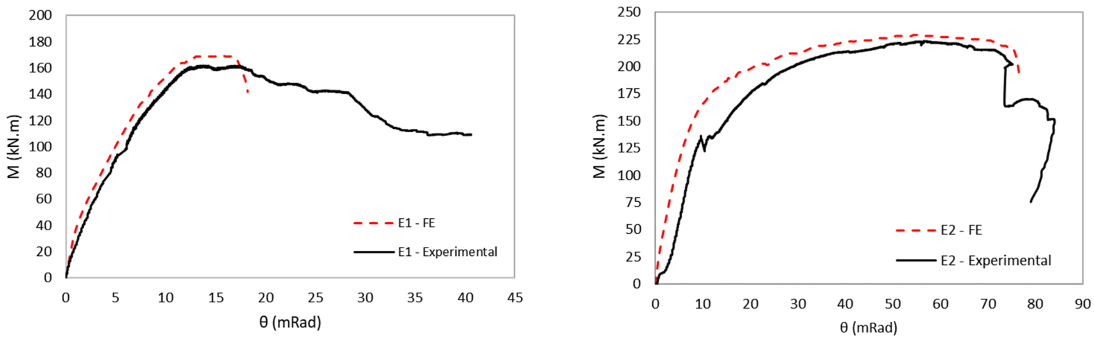


a) b)

Figure 3 – Moment-rotation behavior of composite joint a) E1 test; b) E2 test.

Fig. 4 compares the deformations between the numerical and experimental simulations for E1 test. It can be observed that the failure mode predicted by the numerical model (deformation of the end-plate) was very similar to that observed in the experimental tests.

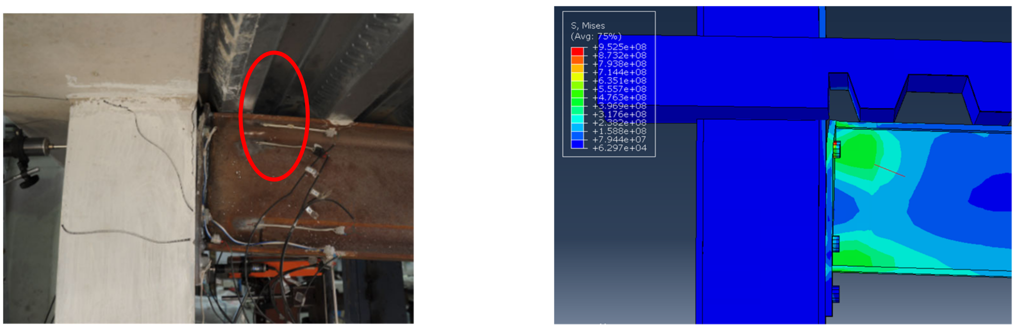


a) b)

Figure 4 – Deformation of end plate a) experimental [9]; b) numerical

The same can be observed for E2 test. The failure occurred in the end-plate and bottom line of high-strength bolts (Fig. 5).

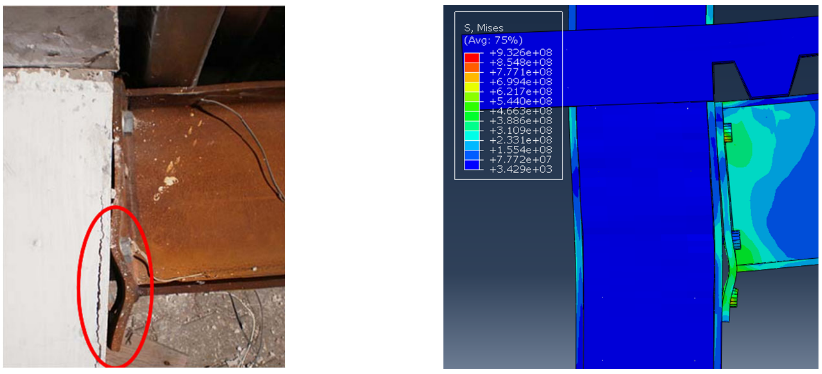

a) b)

Figure 5 – Deformation of end plate and high-strength bolts a) experimental [9]; b) numerical

For the experimental test with cyclic loading, E3 was performed under displacement control with 0.02 mm/s to avoid any acceleration in the specimens. By the same reason, in the numerical simulations, the loading was applied under displacement control. Fig. 6 shows the moment-rotation curve after the cyclic loading. The experimental results showed higher stiffness and load carrying capacity than finite element analysis, due the cyclic hardening. The maximum moment in E3 experimental test was 144 kN.m and the numerical was 135 kN.m.

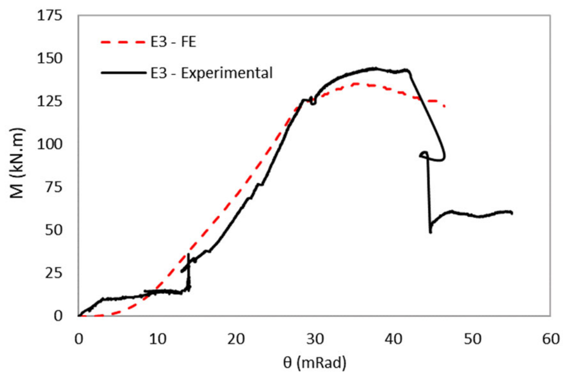


Figure 6 – Moment-rotation behavior of composite joint in E3 test

### 3.2 High Temperature results

The numerical model was also validated for the tests carried out at high temperatures. An additional comparison was carried out with numerical results of Matias et al [10] (Fig. 7). In this case, the joint was heated up to 600 °C and then subject to failure test. The experimental results for the E5 test showed a little bit higher stiffness that can be also explained by the cyclic hardening, which was not taken into account in the numerical model (Fig. 8). The maximum moment observed during the experiment was 72 kN.m and the maximum moment predicted by the numerical model was 69 kN.m, a difference of 4.34%.

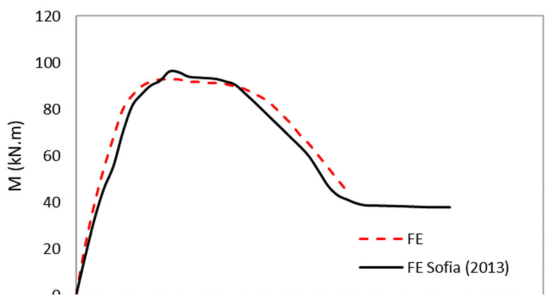


Figure 7 – Moment-rotation behavior of composite joint after fire – comparison with Matias et al [10]

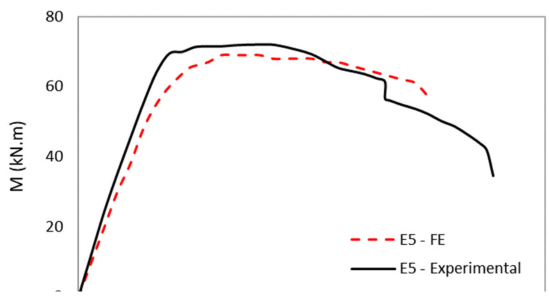


Figure 8 – Moment-rotation behavior of composite joint in E5 test

# 4 Conclusions

This paper presented the results of a validation of a finite analysis of composite steel and concrete joint subjected to a fire after seismic loading. The proposed model was validated with experimental results carried out by Barata et al. [9] and numerical results of Matias et al. [10]. The results were similar with little error in the prediction of the loadbearing capacity and stiffness. However, the numerical model was capable to predict the failures modes accurately. Thus, it is possible to conclude that the numerical model is capable of predicting the behavior of composite steel and concrete joints with end-plate subjected to post-earthquake fire. This model is now being used in a parametric study, varying different parameters, such as the load level, fire curve, geometry of the model, etc., in order to find behavioral parameters for this type of joints in case of fire after earthquake.

## Acknowledgements

The authors would like to thank the support under the research project PCIF/MOS/0129/2018 - Interdisciplinary Methodologies for Protecting Industrial Zones Against Forest Fires, financed by the Portuguese Foundation for Science and Technology.

## References

[1] Ferro, C. C. Earthquake in Lisbon, tremor in Bahia: a protest against the donation for the reconstruction of Lisbon (1755-1757). MSc Thesis in Social History, Niteroi-RJ: Federal University Fluminense, 2009. 153 p. (in Portuguese)

[2] Schencking, C. (2013). The Great Kanto Earthquake and the Chimera of National Reconstruction in Japan. *Columbia University Press*. 400p.

[3] National Achieve (2023). San Franscisco earthquake of 1906. United Kingdom: Encyclopaedia Britannica. https://www.britannica.com/event/San-Francisco-earthquake-of-1906 [accessed on: 11 April 2023].

[4] National Fire Protection Association (2015). Fire history: Kobe earthquake and fire. https://www.nfpa.org/news-and-research/publications-and-media/blogs-landing-page/nfpa-today/blog-posts/2015/01/17/fire-history-kobe-earthquake-and-fire [accessed on 28 March. 2023].

[5] Nuclear regulatory commission (2015). Japan's Fukushima Daiichi ET Audio File. Neal R. Gross. https://www.nrc.gov/docs/ML1205/ML12052A106 [accessed on: 15 April. 2023].

[6] Tartaglia, R. D'Aniello, M. Wald, F. (2021). Behaviour of seismically damaged extended stiffened end-plate joints at elevated temperature*. Engineering Structures 247.* https://doi.org/10.1016/j.engstruct.2021.113193

[7] Xu, J. et al. (2021). Post-earthquake fire resistance of bolted end-plate connection joint with end-plate and web stiffeners. Journal of Constructional Steel Research 185. https://doi.org/10.1016/j.jcsr.2021.106835

[8] Song, Q.; Heidarpour, A; Zhao, X; Han, L. (2016) Post-earthquake fire behaviour of welded steel I-beam to hollow column connections: An experimental investigation. *Thin-Walled Structures*. p 143-153. https://doi.org/10.1016/j.tws.2015.03.032.

[9] P. Barata. (2010). Behaviour of Composite Steel and Concrete Joints subjected to Fire after Earthquake. MSc Thesis. University of Coimbra, Portugal. (in Portuguese)

[10] A, Matias. (2013). Numerical Modelling of Composite Steel and Concrete Joints subjected to Fire. MSc Thesis. University of Coimbra, Portugal. (in Portuguese)

[11] EN 1993:1-1, Eurocode 3: Design of steel structures – Part 1-2: Structural fire designs. CEN Brussels (2005).

[12] F. Hanus; G. Zilli; J. M. Franssen. Behaviour of Grade 8.8 bolts under natural fire conditions – Tests and model. *Journal of Constructional Steel Research,* vol 8, pp. 1292-1298. 2011. https://doi.org/10.1016/j.jcsr.2011.03.012.

[13] H. Katabdari; A. Daryan; N. Hassani. Predicting post-fire mechanical properties of grade 8.8 and 10.9 steel bolts. *Journal of Constructional Steel Research,* vol. 162. 2019. https://doi.org/10.1016/j.jcsr.2019.105735.

[14] EN 1992:1-2, Eurocode 2: Design of concrete structures – Part 1-2: General rules – Structural fire design. CEN Brussels, 2004.

[15] H. Silva (2013). Numerical simulation of the behavior of crestbond shear connectors. Federal University of Viçosa, Viçosa, Brazil. (in Portuguese)

[16] F. Bolina. (2021). Analysis of the Effect of the Continuity on Composite Steel Decking Slabs in case of Fire. University of Vale do Rio dos Sinos, São Leopoldo, Brazil. (in Portuguese).

[17] European Convention for Constructional Steelwork, 1986, Recommended Testing Procedure for Assessing the Behavior of Structural Steel Elements under Cyclic Loads, ECCS Publication No. 45.